Crystal Structures of KDOP Synthase in Its Binary Complexes with the Substrate Phosphoenolpyruvate and with a Mechanism-Based Inhibitor[†,‡]

Oluwatoyn Asojo,[§] Jonathan Friedman,*[,§] Noam Adir,[∥] Valery Belakhov,[∥] Yuval Shoham,[⊥] and Timor Baasov*[,∥]

Department of Chemistry, University of Houston, Houston, Texas 77204-5641, and Department of Chemistry and Institute of Catalysis Science and Technology and Department of Food Engineering and Biotechnology, Technion, Haifa 32000, Israel

Received February 16, 2001; Revised Manuscript Received March 5, 2001

ABSTRACT: The crystal structures of 3-deoxy-D-*manno*-2-octulosonate-8-phosphate synthase (KDOPS) from *Escherichia coli* complexed with the substrate phosphoenolpyruvate (PEP) and with a mechanism-based inhibitor (K_d = 0.4 μM) were determined by molecular replacement using X-ray diffraction data to 2.8 and 2.3 Å resolution, respectively. Both the KDOPS·PEP and KDOPS·inhibitor complexes crystallize in the cubic space group *I*23 with cell constants $a = b = c$ = 117.9 and 117.6 Å, respectively, and one subunit per asymmetric unit. The two structures are nearly identical, and superposition of their Cα atoms indicates an rms difference of 0.41 Å. The PEP in the KDOPS·PEP complex is anchored to the enzyme in a conformation that blocks its *si* face and leaves its *re* face largely devoid of contacts. This results from KDOPS's selective choice of a PEP conformer in which the phosphate group of PEP is extended toward the *si* face. Furthermore, the structure reveals that the bridging (P−O−C) oxygen atom and the carboxylate group of PEP are not strongly hydrogen-bonded to the enzyme. The resulting high degree of negative charge on the carboxylate group of PEP would then suggest that the condensation step between PEP and D-arabinose-5-phosphate (A5P) should proceed in a stepwise fashion through the intermediacy of a transient oxocarbenium ion at C2 of PEP. The molecular structural results are discussed in light of the chemically similar but mechanistically distinct reaction that is catalyzed by the enzyme 3-deoxy-D-*arabino*-2-heptulosonate-7-phosphate synthase and in light of the preferred enzyme-bound states of the substrate A5P.

The enzyme 3-deoxy-D-*manno*-2-octulosonate-8-phosphate (KDOP)[1] synthase (KDOPS) (EC 4.1.2.16) catalyzes the condensation reaction between D-arabinose-5-phosphate (A5P) and phosphoenolpyruvate (PEP) to form KDOP and inorganic phosphate (P_i, Scheme 1) (*1*). This enzymatic reaction plays an essential role in the assembly process of lipopolysaccharides of most Gram-negative bacteria and is therefore an attractive target for the design of novel antibacterial drugs (*2*). Interestingly, KDOPS belongs to a family of PEP-utilizing enzymes, two of which—UDP-GlcNAc enolpyruvoyl transferase (*MurZ*) and 5-enolpyruvoylshikimate-3-phosphate synthase (EPSPS)—are targeted

Scheme 1: Proposed Mechanism for the KDOPS-Catalyzed Reaction

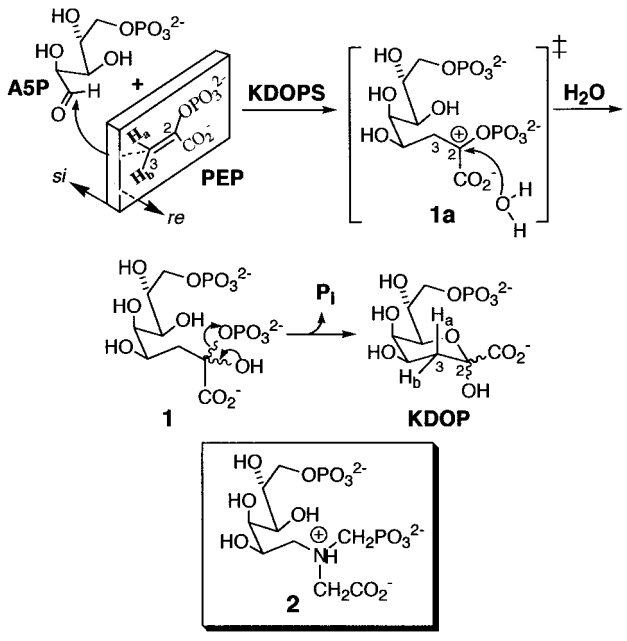

[†] This research was supported by U.S.-Israel Binational Science Foundation Grant 97-356 (T.B. and J.F.), by the Foundation for Promotion of Research at the Technion (T.B.), by the University of Houston Institute for Molecular Design, Keck Center for Computational Biology, and the Environmental Institute of Houston (J.F.), and by the Center of Absorption in Science, Ministry of Immigration Absorption and the Ministry of Science and Arts, State of Israel, Kamea Program (V.B.).

[‡] The structural coordinates for the KDOPS·PEP and KDOPS·**2** structures have been deposited in the Protein Data Bank under ID codes 1G7U and 1G7V, respectively.

* Corresponding authors. T.B.: Department of Chemistry, Technion−Israel Institute of Technology, Haifa, 32000 Israel. E-mail: chtimor@tx.technion.ac.il. Fax: (972)-4-823-3735. J.F.: Department of Chemistry, University of Houston, Houston, TX 77204-5641. E-mail: friedman@kitten.chem.uh.edu. Fax: (713)-743-2726.

[§] Department of Chemistry, University of Houston.

[∥] Department of Chemistry and Institute of Catalysis Science and Technology, Technion.

[⊥] Department of Food Engineering and Biotechnology, Technion.

[1] Abbreviations: KDOP, 3-deoxy-D-*manno*-2-octulosonate-8-phosphate; KDOPS, KDOP synthase; PEP, phosphoenolpyruvate; A5P, arabinose-5-phosphate; DAH7PS, 3-deoxy-D-*arabino*-2-heptulosonate-7-phosphate synthase; REDOR, rotational-echo double resonance; *MurZ*, UDP-GlcNAc enolpyruvoyl transferase; EPSPS, 5-enolpyruvoylshikimate-3-phosphate synthase.

10.1021/bi010339d CCC: $20.00
Published on Web 05/05/2001

by the antibiotic fosfomycin and by the herbicide glyphosate, respectively. The last member of this family is 3-deoxy-D-*arabino*-heptulosonate-7-phosphate (DAHP) synthase (DAHPS), which catalyzes a net aldol reaction similar to that of KDOPS, but between PEP and erythrose-4-phosphate (E4P) to produce DAHP (*3*). A unique mechanistic feature shared by the reactions catalyzed by these four enzymes is that while most enzymatic reactions that use PEP as a substrate proceed through cleavage of the high-energy P−O bond ($\Delta G^{\circ\prime} = -14.8$ kcal/mol), the reactions of these four enzymes proceed through the unusual cleavage of the C−O bond of PEP (*4*).

While the mechanisms of EPSPS (*5*) and *MurZ* (*6*), two enolpyruvoyl transferase enzymes, have been characterized unambiguously, some mechanistic details of the reactions catalyzed by KDOPS and DAHPS are still unresolved. Early studies on KDOPS suggested (*7*) that this enzyme acts upon the acyclic form of A5P and demonstrated (*7*) an ordered sequence of substrate binding and product release, with PEP binding before A5P does and with P_i being released prior to KDOP. The condensation step was shown to be stereospecific, with the *si* face of PEP attaching to the *re* face of the carbonyl of A5P (*8*, *9*). More recent studies using rapid-quench techniques (*10*), including the synthesis and evaluation (*11*) of the first acyclic bisubstrate inhibitor (**2**, K_d = 0.4 μM), supported the original hypothesis of Hedstrom and Abeles (*12*), which was that the reaction pathway proceeds through an acyclic bisphosphate intermediate **1** (Scheme 1). Despite all of the above observations, none of the available evidence unambiguously identifies **1** as the true enzymatic intermediate.

Very recently (*13*), we reported the first direct identification of active site residues of KDOPS by solid state, rotational-echo double-resonance (REDOR) NMR, in combination with mutagenesis studies (*14*). In parallel, the first X-ray crystal structure of KDOPS at 2.4 Å resolution was reported (*15*). This study demonstrated that the enzyme is a homotetramer in which each monomer has the fold of a $(\beta/\alpha)_8$ barrel, similar in many respects to the previously solved X-ray structure of DAHPS (*16*). These earlier KDOPS crystals were grown in the presence of 1.4 M $(NH_4)_2SO_4$ and 0.4 M $(K/H)_3PO_4$, and had two SO_4^{2-}/HPO_4^{2-} sites that were identified in the structure. These were interpreted as occupying the phosphate positions of the substrates, PEP and A5P. On the basis of this interpretation, a model structure for the active site of KDOPS was proposed in which the phosphate groups of PEP and A5P are 13.0 Å apart, allowing KDOP synthesis to proceed via an *acyclic* intermediate **1**.

Using molecular replacement, Kretsinger and co-workers (*17*) have recently solved another structure of *Escherichia coli* KDOPS at 3.0 Å resolution. Although in this case the crystals were grown in poly(ethylene glycol) (PEG) 1500 in the presence of both substrates, PEP and A5P, neither the enzyme-bound PEP nor the bound A5P or the product KDOP could be identified. Two phosphate peaks were found in this structure as well, only 10.3 Å apart, in contrast to the distance of 13.0 Å found in the structure of Radaev et al. (*15*).

As part of our study on the structure−function relationship of KDOPS, we report here the first crystal structures of the *E. coli* KDOPS in binary complexes with the substrate PEP and with the mechanism-based inhibitor **2** at 2.8 and 2.3 Å resolution, respectively. These structures provide important information about the enzyme active site architecture and about the interactions between the substrates and the enzyme. Some important mechanistic implications of these observations are discussed.

MATERIALS AND METHODS

Protein Purification and Crystallization. The wild-type KDOPS (specific catalytic activity 9 units/mg) was isolated from the overproducing *E. coli* DH5α (pJU1) strain, as previously described (*7*). For the production of selenomethionine-labeled KDOPS ([Se-Met]KDOPS), competent *E. coli* methionine auxotroph cells [strain B834(λDE3) (Novagen)] were transformed with plasmid pJU1 containing the *kdsA* gene. Using the protocol of optimization of growth conditions developed in this laboratory (*18*), we observed that over 100 mg of homogeneous [Se-Met]KDOPS could be obtained per liter of culture. The molecular mass difference between [Se-Met]KDOPS (31 311.46 ± 8.66) and the native KDOPS (30 842.38 ± 4.97) was determined to be 470.8 mass units (VG BioQ electrospray spectrometer), indicating 100% substitution of Met with Se-Met residues. The k_{cat} value for [Se-Met]KDOPS (5.3 s^{-1}) was about 29% lower than that of the native enzyme (7.1 s^{-1}) (*7*). Both the native and the [Se-Met]KDOPS exhibited similar K_m values for PEP binding (7.1 and 7.9 μM, respectively). These kinetic data clearly demonstrate that the incorporation of Se-Met into KDOPS does not significantly alter either KDOPS's catalytic activity or its substrate specificity.

Purified [Se-Met]KDOPS was dialyzed against 0.1 M Tris-HCl buffer (pH 7.2) containing 0.02% β-mercaptoethanol and 0.02% sodium azide, for three changes over 12 h, and was then concentrated to about 45 mg/mL with an Amicon Centricon-10 microconcentrator. All crystals were grown at 23 °C by vapor diffusion in hanging drops. Drops were prepared by mixing 2 μL of the above concentrated enzyme solution with 2 μL of the reservoir solution. The reservoir solution contained either inhibitor **2** (0.053 mM) or the substrate PEP (10 mM) in sodium 2-(*N*-morpholino)ethanesulfonate (MOPS) buffer (61 mM, pH 6.1) with glycerol (25% v/v) as cryosolvent and PEG 400 (10% v/v).

Cubic crystals of the [Se-Met]KDOPS·PEP complex in the space group *I*23, with cell constants $a = b = c = 117.9$ Å and $\alpha = \beta = \gamma = 90°$, appeared within several days. Crystals were flash frozen in a stream of N_2. X-ray data extending to 2.8 Å were collected at −180 °C using the inverse-beam method on an R-axis II imaging plate system. A complete set of data was collected from a single crystal.

The crystals of the [Se-Met]KDOPS·**2** complex also belong to the space group *I*23 with cell constants $a = b = c = 117.6$ Å and $\alpha = \beta = \gamma = 90°$. X-ray data extending to 2.3 Å were collected at −180 °C at an energy of 12 660 eV on Beamline X4A at the Brookhaven National Synchrotron Line Source. This Se-Met MAD (multiple wavelength anomalous diffraction) data set could not be used to determine MAD phases because of missing data at other wavelengths. X-ray data sets were processed using the programs DENZO (*19*) and SCALEPACK (*20*). The structure was solved by molecular replacement using AMORE (*21*) with the ligand-free structure of KDOP synthase (*15*) (subunit A) as the search model. The crystallographic model was refined using X-PLOR (*22*).

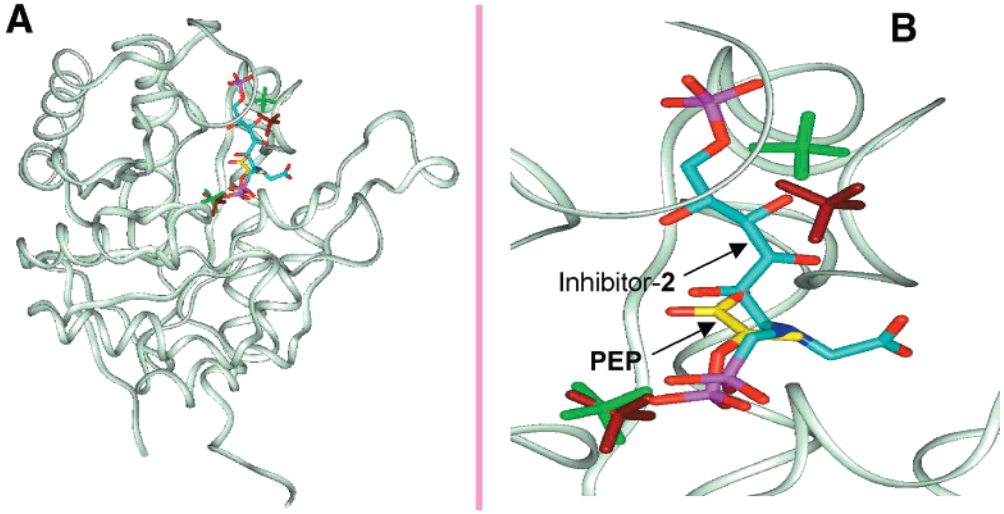

FIGURE 1: Superposition of the KDOPS·PEP and KDOPS·**2** structures, the Radaev et al. (*15*) KDOPS structure (PDB code 1D9E, subunit a), and the Wagner et al. (*17*) KDOPS structure (PDB code 1GG0). (A) The main chains of all four overlapped KDOPS structures are almost identical, and therefore only the KDOPS·**2** chain is shown in beige ribbon form for clarity. The two phosphate/sulfate ions proposed to bind to the A5P−phosphate position (at the top of the protein) and the PEP−phosphate position (in the middle of the protein) are depicted in green and brown for the 1D9E and 1GG0 structures, respectively. Carbon backbones of the PEP and inhibitor (**2**) molecules are shown in yellow and cyan, respectively, while oxygens, nitrogens, and phosphorus atoms are shown in their default CPK colors. (B) Magnified view of the overlapped ligands and phosphate/sulfate ions in the active site. Colors are as described in panel A. The phosphate/sulfate distances are 12.11 and 10.32 Å for the 1D9E (subunit a) and 1GG0 structures, respectively, while the phosphate−phosphonate distance in the KDOPS·**2** structure is 11.69 Å. All illustrations were prepared using InsightII (Molecular Structure Inc.).

RESULTS

Since the molecular structure of **2**, the most potent competitive inhibitor known to date ($K_d = 0.4\ \mu M$), combines the key features of both substrates PEP and A5P into a single molecule (Scheme 1), the structural data for the KDOPS·PEP and KDOPS·**2** complexes that were obtained in this study are likely indicators of the identity of active site residues that participate in the recognition of both natural substrates by KDOPS. Analysis of these structures also provides an important basis for understanding how KDOP's three-dimensional structure dictates its catalytic mechanism.

Overall Structure. In the structures of the KDOPS·PEP and KDOPS·**2** complexes, the enzyme is present as a tetrameric complex, one subunit in the asymmetric unit, confirming the conclusion of Radaev et al. about the tetrameric nature of KDOPS (*15*). While the overall $(\beta/\alpha)_8$ barrel structures reported here (Figure 1A) are very similar to those reported earlier, for our crystal forms, all of the amino acid residues were visible and could be identified. Two peptide loops that were missing in the molecular replacement search model (Asp208−Gly216 and Ala247−Gly251, an active site strand) were identifiable in $F_o - F_c$ difference maps and could be traced (Figure 2). The two structures presented in this report are almost identical with each other (rmsd values of 0.41 or 0.45 Å for α-carbons or all atoms, respectively). The two structures are also very similar to the two previously solved structures: the rmsd values are 1.3 Å for all comparable α-carbon atoms, when our structures are aligned with the structure of Radaev et al. (*15*) or with the structure of the Wagner et al. (*17*). However, since our structures are both more complete and contain bound substrate/inhibitor, when these regions of the protein are not included in the calculation, the α-carbon rmsd for the remaining 91% of the protein is 0.70 Å. A number of critical residues occupy significantly different positions, and these shifts are necessary to accommodate the presence of the substrate and inhibitor molecules in our structures (Figure 3). In particular, a featureless strand near the active site appears to adopt a more helical conformation in our structure. Other major differences arise (1) in surface loops, (2) in the interdomain strand region at the C-terminus, and (3) in the amino acid residues immediately adjacent to the unobserved, disordered segments of the previous structures. Following coordinate refinement by simulated annealing and conjugate gradient minimization (Table 1), the interactions between the substrates and active site residues could be identified in our structure. Several residues near the A5P portion of the active site retain high-temperature factors, indicating the flexibility of this region. The active site can be described as a long narrow cleft in the center of the β_8 barrel (Figure 1). The cleft is shallowest in the A5P−phosphate binding site and becomes progressively deeper toward the PEP−phosphate binding site.

KDOPS−PEP Interactions. The closest contacts of KDOPS with PEP appear to be salt bridges that form between the phosphate oxygens and Arg168 and His202, while Lys138 and Gln141 form longer range electrostatic contacts (Figure 4A). The carboxylate group of PEP lies between His202 and Asn62 and points into the cleft toward the A5P binding site. Radaev et al. (*15*) proposed that three lysine residues (Lys55, Lys60, and Lys138) might interact with the carboxylate group of PEP; however, at the present level of detail, these three residues are all too distant for the formation of hydrogen bonds to the carboxylate of PEP. The vinyl group of PEP points outward from the active site cleft and is not within van der Waals contact distance of any nearby residue. The phosphate/sulfate ions in the Radaev et al. (*15*) and Wagner et al. (*17*) structures are about 3.3 Å away from the PEP−phosphate and are more deeply buried in the active site cleft (Figure 1B).

*KDOPS−**2** Interactions.* The structure of **2** is comprised of three unique molecular fragments: the phosphonate group,

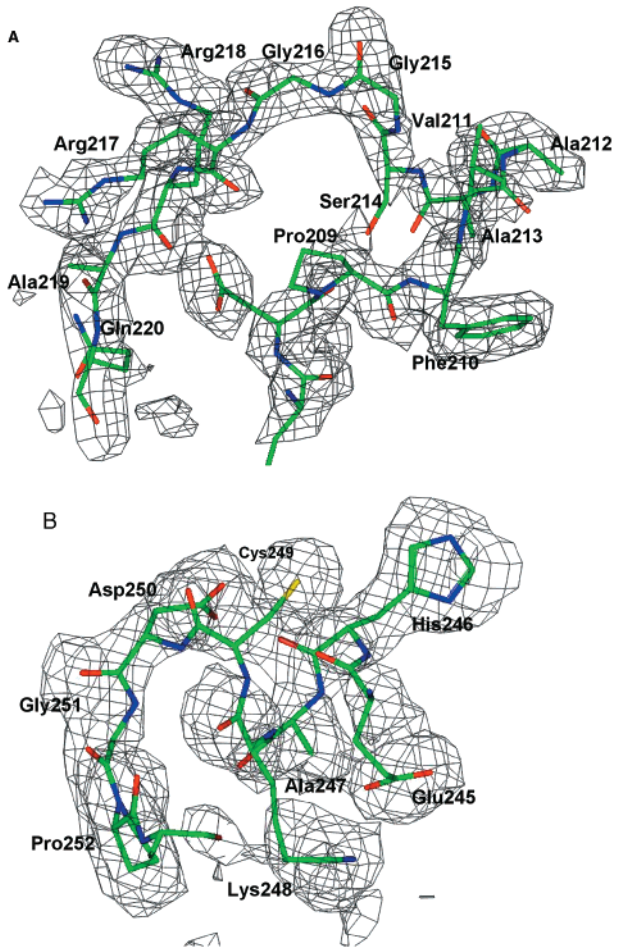

FIGURE 2: Omit maps of the refined coordinates of two loops in the KDOPS·PEP structure not present in the original molecular replacement search model (1D9E, subunit A). The two loops added in the KDOPS·PEP and KDOPS·**2** structures include residues 206−217 (panel A) and 245−252 (panel B). Following positioning of the sequence in unrefined electron density maps and refinement of the structure, $F_o - F_c$ omit maps were calculated to ensure proper positioning.

the carboxylate group, and the A5P group (Figure 1B). The distance between the two phosphorus atoms of **2** in the structure of the KDOPS·**2** complex is 11.8 Å. This value is intermediate between those observed for the corresponding interanionic distances (phosphate/sulfate ions) in the structure of Radaev et al. (*15*) and in that of Wagner et al. (*17*) (Figure 1). It is not unexpected that the observed positions of ions bound at higher ionic strength may vary slightly upon observation at reduced ionic strength and in the presence of additional constraints imposed by the remainder of the substrate. The similar general location of bound anions on the surface of the enzyme, under the variety of experimental conditions, further accentuates the positive electrostatic potential that must be present in this cavity (*15*, *17*). The phosphonate group of **2** is bound between residues Arg168, Asn141, and His202 (Figure 4B). In the KDOPS·**2** complex, residues Lys138 and Arg168 occur in different orientations than they do in the KDOPS·PEP complex. In the present KDOPS·**2** complex, N_δ of Arg168 lies most closely to the peripheral oxygen atom of the phosphonate group of **2**, with Lys138 directed away from this phosphonate group. In the KDOPS·PEP complex, one peripheral phosphate oxygen atom interacts with the peripheral N_ζ of Arg168 and a second oxygen atom is within 3.8 Å of N_ϵ of Lys138 (Figure 4).

The A5P portion of **2** is stretched along the cleft, exhibiting many van der Waals contacts with the protein. Residue Arg63 contacts this sugar portion extensively, folding over the carbon chain of the sugar and shielding sugar carbon atoms corresponding to C4 and C5 of A5P nearly completely from the solvent. Carbon atoms C1 and C2 of A5P are relatively open to the solvent on one face of **2**. The phosphate group of **2**, corresponding to that of A5P−phosphate, is in close contact with the guanidino group of Arg63 (Figure 4B). The conformation of this side chain differs significantly between the KDOPS·**2** and KDOPS·PEP complexes (Figure 3). Residue Ser64 (not shown) is about 5 Å away from the closest phosphate oxygen of **2** and does not appear to interact with the A5P fragment of **2**, in contrast to earlier indications by Radaev et al. (*15*). The phosphate/sulfate ions in the Wagner et al. (*17*) structure are positioned quite differently than the phosphonate and phosphate groups of the inhibitor **2**. The anion in the structure of Wagner et al. (*17*) that corresponds most closely to the phosphate group of A5P lies almost completely outside the cleft, nearly 6 Å away from corresponding phosphate in the structure of the KDOPS·**2** complex (Figure 1B).

Water. The positions of 15 and 21 ordered, protein-bound water molecules were found in the structures of the KDOPS·PEP and KDOPS·**2** complexes, respectively. A single water molecule in the structure of the KDOPS·**2** complex is within hydrogen-bonding distance of Asn62 (data not shown), which is the only protein residue that is even remotely close to the *re* face of the PEP moiety of **2**. The absence of a water molecule positioned more closely to C2 of PEP may indicate that this water molecule, which is mechanistically required for nucleophilic attack, may be disordered in the KDOPS·PEP structure (see the Discussion section).

DISCUSSION

The structural information achieved in this study confirms in many aspects the recently reported substrate-free structures of KDOPS (*15*, *17*). However, major differences are observed in the conformations of the active site residues responsible for the binding of both the PEP and A5P substrates (Figure 1). Visualization of the PEP and inhibitor **2** in our structures allows us to rationalize the chemically determined stereochemical course of the enzyme-catalyzed reaction (*8*, *9*). The results of such analysis lead to important implications about the mechanism of action of KDOPS.

Stereochemical Control at the PEP Binding Site. The strong, well-defined electron density in the map of the KDOPS·PEP complex (Figure 4A) clearly defines the positions of the two vinylic carbon atoms and of phosphate and carboxylate groups of the enzyme-bound PEP. Inspection of the PEP binding site shows that PEP contacts the protein predominantly through its peripheral phosphate oxygen atoms, with this phosphate group anchored to the enzyme in a configuration that blocks the *si* face of the PEP and leaves the *re* face of PEP largely devoid of close contacts. By analogy with other small, highly charged substrates, this suggests that the driving force for substrate binding is largely electrostatic with substantial contributions to the free energy of interaction arising from the release of water from the solvation sphere of PEP upon going from its free to its enzyme-bound form.

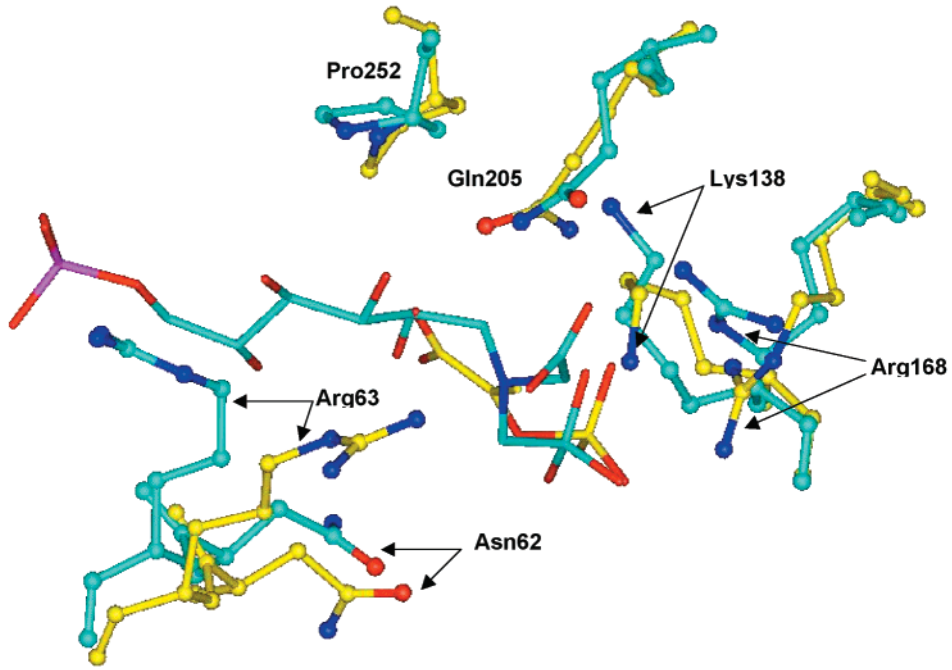

FIGURE 3: Positions of active site amino acid residues which have significant conformational changes upon replacement of the substrate PEP (from the KDOPS·PEP structure, yellow) with the inhibitor **2** (from the KDOPS·**2** structure, cyan). Oxygens (red), nitrogens (blue), and phosphorus (magenta) atoms are colored to clarify the side chain positions.

Table 1: Diffraction Data and Refinement Statistics

	KDOPS·PEP	KDOPS·**2**
diffraction data		
space group	*I*23	*I*23
cell dimensions	$a = 117.9$	$a = 117.6$
resolution (Å)	20−2.8	20−2.23
outer shell resolution (Å)	2.9−2.8	2.3−2.23
R_{merge} (%)	6.6	9.1
redundancy		
overall I/σ	6.9 (3.2)[a]	17.1 (2.8)[a]
completeness (%)	85.8 (85.3)[a]	70.6 (14.1)[a]
no. of residues	248	248
no. of protein atoms	2193	2193
no. of nonprotein atoms		
water	15	31
ligand	10	25
refinement statistics		
no. of reflections		
working *R* set	6494	7164
free *R* set	317	360
I/σ cutoff	3.0	3.0
resolution (Å)	8−2.8	8−2.3
R-factor (%)	22.8	22.5
free *R*-factor (%)	28.1	25.9
geometry		
rmsd from ideality		
bond length (Å)	0.016	0.017
bond angles (deg)	2.5	2.4
improper angles (deg)	2.3	2.2
dihedral angles (deg)	26.1	25.7

[a] Statistics for outer shell reflections.

Two features of PEP's interaction with the enzyme are of importance. First, while the carboxylate oxygen atoms, the bridging oxygen atom of the phosphate, and all three of the carbon atoms are coplanar, the phosphate group extends from this plane toward the *si* face of the PEP molecule (Figure 4A and Figure 5A). Such a distinct conformational selectivity of KDOPS in its recognition and binding of PEP is likely to be of some mechanistic significance. Indeed, the bridging oxygen atom (P−O−C) appears not to be strongly hydrogen-bonded. All possible contacts of this P−O−C oxygen atom—those with O_δ of Asn62 (4.3 Å and toward the *re* face of PEP), $N_{\eta 2}$ of Arg168 (4.48 Å and toward the *si* face), and N_δ of His202 (4.36 Å and toward the *si* face)—are too far or are apparently in unfavorable orientations for hydrogen bonding (Figure 4A). This lack of direct contact to the P−O−C oxygen atom, resulting in an electron-rich bridging oxygen, may serve to favor nucleophilic attack by C3 of the vinylic double bond of PEP onto the electrophilic C1 atom of A5P (Figure 5A). The observed conformer is also in complete accord with the observed stereochemical course of the condensation step (*8*, *9*). That is, the observed addition by the *si* face of PEP to the *re* face of the carbonyl of A5P may be rationalized by the enzyme-mediated direction of one of the lone pair sp^3 orbitals of the bridging oxygen to be antiperiplanar relative to the newly generated C−C bond (*23*). *Thus by stabilizing the observed conformer of bound PEP, the enzyme may activate the C3 atom of PEP to be more nucleophilic*. This, indeed, can only be achieved by the conformer given in Figure 5A, while its opposite conformer (Figure 5B) would lead to addition to the wrong (i.e., *re*) face of PEP.

A second important feature of the interaction of PEP with KDOPS arises from how PEP's carboxylate group interacts with the protein. This carboxylate group is distant from the nearest protein residues. Atom O1′ of the carboxylate is 4.0 Å away from either nitrogen atom N_ϵ or N_δ of His202. Atom O2′ lies 3.8 and 3.6 Å away from these nitrogen atoms and lies 4.3 Å away from N_ϵ of Gln205 (Figure 4A). Additionally, the positive charge of His202 is largely compensated by its interaction with the anionic phosphoryl group. All of these observations suggest that the carboxylate group of PEP should bear a full, albeit delocalized negative charge. Two important mechanistic advantages may be drawn from this implied ionization state of the carboxylate group of enzyme-bound PEP.

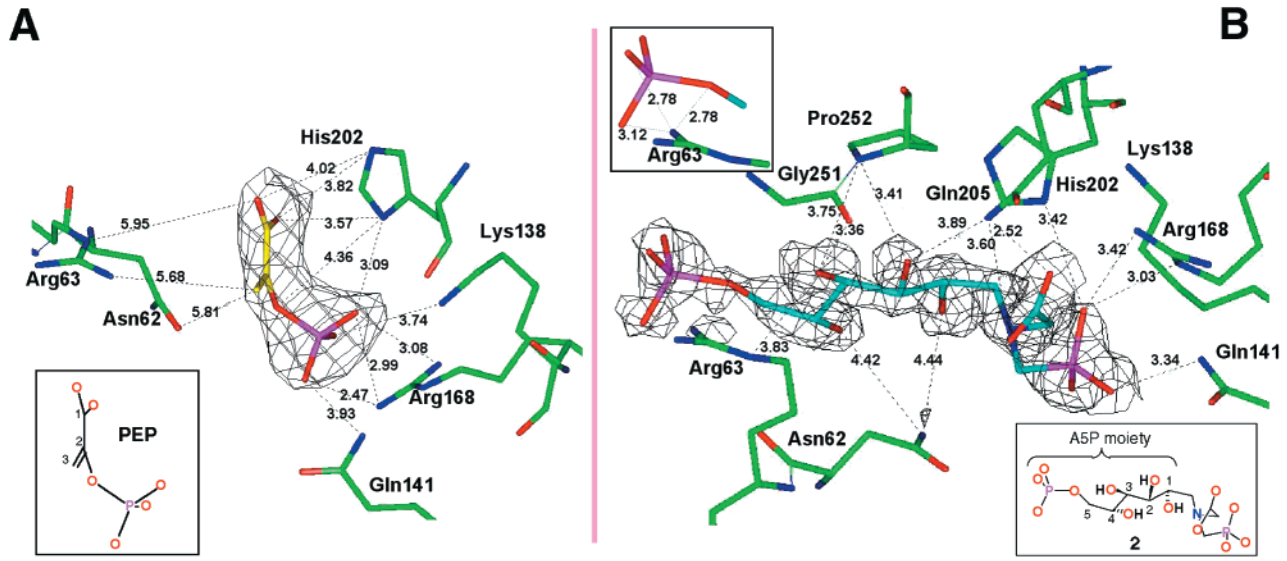

FIGURE 4: Interactions within the KDOPS active site. (A) Interactions between KDOPS amino acid residues and PEP in the KDOPS·PEP crystal structure. PEP carbon atoms are in yellow; all other atoms are colored according to the CPK scheme. A section of a $F_o - F_c$ electron density omit map, contoured at 1.5σ, shows unambiguous density for the PEP molecule in the configuration shown. Residues Asn62 and Arg63, which interact weakly with the PEP substrate, are depicted to show the difference between the tight contact with PEP's *si* face and the weaker contact with the *re* face. (B) Interactions between KDOPS residues and inhibitor **2** (cyan carbon atoms) in the KDOPS·**2** structure. A section of a $F_o - F_c$ electron density omit map, contoured at 1.0σ, shows unambiguous density for **2**. Strong contacts between the protein and **2** are seen on both phosphate and phosphonate ends and with the carboxyl group.

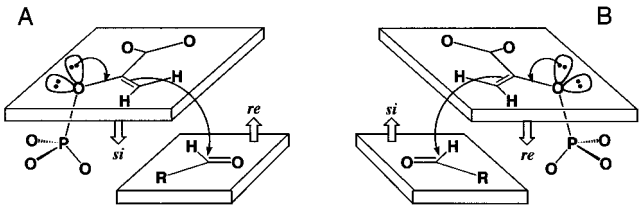

FIGURE 5: Two conformers of PEP. The phosphate PO_3 group extends from the plane of the PEP molecule either toward the *si* face (A) or toward the *re* face (B). One of the lone pair orbitals of the bridging (P−O−C) oxygen is oriented to either the *re* face (A) or the *si* face (B) of the molecule so that is antiperiplanar relative to the newly generated C−C bond between C3 of PEP and the C1 aldehyde of A5P. The R group represents the remaining sugar portion of A5P.

The first such advantage is that the inductive electron-donating character (*24*) of the negatively charged carboxylate group is expected to *increase* the nucleophilicity of the double bond of PEP, an important requirement for the first event of the coupling step. Neutralization of the charge of PEP's carboxylate group (e.g., through either strong hydrogen-bonding or salt-bridging interactions) would have led to a strong decrease in the nucleophilicity of the double bond due to the electron-withdrawing character of "neutral" carboxylic acid (*24*). The strongly reduced nucleophilicity of the olefin in the neutral carboxylic acid form of PEP is independently indicated (1) by the prior observation that the enolic O−C2 bond exhibits partial double bond character in several different small molecule crystal structures of monoionized PEP (*25*) and (2) by crystal structure analysis of the enolase-catalyzed transformation of PEP to 2-phospho-D-glycerate (PGA) (*26*). In this enolase reaction, the negatively charged carboxylate group of PEP is strongly neutralized by a catalytic Mg^{2+} ion situated at 2.4 Å from both oxygen atoms of the carboxylate group. Such neutralization of the carboxylate charge leads to increased electrophilicity at C3 of PEP and thereby facilitates nucleophilic attack by water at this position.

A second advantage of maintaining a negative charge on the carboxylate group of PEP in the KDOPS reaction is that such negative charge should inductively stabilize the partial positive charge that is present on C2 of PEP in the transition state of the condensation step (**1a**, Scheme 1). Similar rate enhancements due to a negatively charged α-carboxylate group are well documented in the acid-catalyzed hydrolysis of KDO-2-phosphates (*24*). Thus, although at this stage of investigation it is not clear whether the formation of new C−C and C−O bonds during the condensation step is a synchronous or stepwise process, the current results on the position of PEP in its binding pocket would suggest that these processes should occur in a stepwise manner. The initial formation of a transient oxocarbenium intermediate **1a**, or an early transition state having oxocarbenium character, must be followed by the capture of water at the cationic C2 position to complete the formation of acyclic intermediate **1** (Scheme 1). The opposite sequence of steps, the initial nucleophilic attack of water at C2 of PEP and subsequent coupling of carbanionic C3 with the carbonyl of A5P, is very unlikely because it would require a highly activated hydroxide ion and strong neutralization of PEP charges (*26*), which are not observed in KDOPS.

The suggested stepwise mechanism for KDOPS is further indicated by results obtained through mechanistic experiments with **2** (*11*), with analogues of PEP (*27*), and with intramolecular models of the KDOPS-catalyzed reaction (*28*). Furthermore, the same oxocarbenium ion transition state of PEP has been suggested earlier to account for the enzymatic reactions of *MurZ* (*29*) and EPSPS (*30*). These enzymes catalyze the enol ether transfer from PEP to their respective cosubstrate alcohols and represent a different distinct class of enzymatic reaction involving the same C−O bond cleavage of PEP and the same stereospecific 2-*si* face

addition of an electrophile at C3 of PEP, which is observed for KDOPS (*4*).

This commonality in stereochemical course of the reaction further strengthens the mechanistic links between these two distinct classes of enzymes and may also indicate a structural and evolutionary relationship between these two classes (*4*). We therefore suggest that, although PEP-bound structures are not yet available for EPSPS and *MurZ*, the recognition and binding of PEP by these enzymes should resemble that by KDOPS. Moreover, although the C−O bond cleavage of PEP represents an unusual class of PEP reaction, the stereospecific 2-*si* face addition at C3 of PEP is consistent for nearly all PEP-utilizing enzymes, and this poses some intriguing evolutionary questions regarding a common PEP binding motif (*4*, *8*, *13*, *31*). Indeed, a search of 3D structures of PEP-utilizing enzymes in the Protein Data Bank reveals that yeast enolase (*26*), PEP-carboxylase (PEPC) (*32*), pyruvate kinase (PK) (*33*), and pyruvate phosphate dikinase (PPDK) (*34*) all have similar PEP binding domains that form an α/β barrel. While it had only been clearly demonstrated that PEP binds to enolase with its phosphate group extending from the *si* face (*26*) (Figure 5A), model studies with metal-bound PEPC, PK, and PPDK also predict the identical binding mode for PEP with these enzymes (*32*).

Surprisingly, in contrast to the similarities observed within the other class of PEP-utilizing enzymes, comparison of the KDOPS-bound PEP to the PEP molecule bound by the structurally and mechanistically most closely related enzyme, DAHPS, reveals that DAHPS binds to the opposite conformation of PEP (Figure 5B) (*16*). Although the latter structure was determined for the DAHPS·PEP·Pb^{2+} complex, in which the conformation of PEP may be dramatically perturbed by the unique chemical properties of Pb^{2+} (*16*), it is clear that resolution of this apparent discrepancy between the binding of PEP by KDOPS and by DAHPS awaits further experiments.

Catalytic Strategies of KDOPS and DAHPS. The recent insightful analysis of the structural and evolutionary relationship between KDOPS and DAHPS led Radaev et al. (*15*) to conclude that these proteins evolved from a common ancestor and that they follow identical catalytic strategies. In contrast, on the basis of the different structural motifs for the recognition and binding of PEP by these two enzymes, we suggest that the initial elementary steps of their catalytic mechanisms might be also very different. Indeed, earlier studies by DeLeo et al. (*35*) and recently by Wagner et al. (*36*) have suggested that C2 of PEP serves as an electrophilic center in the DAHPS-catalyzed reaction. Regiospecific attack by water at this center was proposed to be the initial catalytic step, followed by addition by C3 of PEP to C1 of E4P. This mechanism differs from that in the KDOPS reaction, in which C3 of PEP instead appears to function as a nucleophile in the first step. Thus, the functioning of PEP either as a C2 electrophile (in DAHPS) or as a C3 nucleophile (in KDOPS) must be exquisitely controlled by the interaction of PEP with these enzymes. This postulated mechanistic difference between these two enzymes—despite the apparent chemical similarity in the catalyzed reactions—in fact can rationalize the unique requirement for metal ions by DAHPS, but not by KDOPS (*1*). However, it is clear that the complete resolution of this issue awaits further structural and mechanistic characterization of both enzymes and of site-directed mutants of these enzymes.

The A5P Binding Site. Previous studies have demonstrated that KDOPS acts upon the acyclic (aldehyde) form of A5P (*7*) and that initial binding of either PEP or A5P leads to kinetically competent catalysis (*10*). In addition, the recent solid-state REDOR NMR data (*14*) on the binary KDOPS·A5P complex strongly suggested that both the α- and β-furanose forms of A5P, which constitute more than 97% of its anomers in solution, are the primary forms which bind to KDOPS. The rationalization for these accumulated observations was that bound cyclic A5P should be able to open up to its acyclic form before the chemistry of the C−C coupling step occurs. The structural data that we present here for the A5P region of the KDOPS·**2** complex strongly support this assumption.

First, while the two hydroxyl groups corresponding to C2−OH and C3−OH of the A5P portion of the inhibitor are close to or within hydrogen-bonding range of a few possible hydrogen bond donors and acceptors on the enzyme, two other hydroxyl groups corresponding to C1−OH and C4−OH have no neighboring hydrogen-bonding atoms from the protein closer than 4 Å away (Figure 4B). The structure implies that, aside from the ionic interactions with the C5−phosphate group, the C2−OH and C3−OH may participate in recognition of A5P through possible hydrogen-bonding interactions. The C4−OH participates through a van der Waals contact with C_β of Asn62, and the involvement of the C1−OH appears to be less direct. In general, much, though not all, of the A5P portion of **2** fits rather snugly into the active site pocket, indicating a large degree of van der Waals contact. This suggests that much of the free energy of interaction of A5P with KDOPS may be entropic in origin, arising from the release of water from the hydration zone of free A5P, again a common situation for small hydrophilic ligands. Thus the orientation of A5P appears to be driven by electrostatic and complementary van der Waals interactions with the protein.

The results of some earlier experimental observations of the interactions of deoxy analogues of A5P with KDOPS can be rationalized with regard to the geometry of this interaction surface. The analogue 4-deoxy-A5P serves as a substrate with a k_{cat} value that is similar to that of A5P (*7*), while 2-deoxy-A5P and 3-deoxy-A5P do not function either as substrates or as inhibitors of the enzyme (*37*). The hydroxyl groups corresponding to C2−OH and C3−OH of A5P both interact predominantly with the one peptide turn (residues Gly151−Pro152) that becomes ordered in the structures of both the PEP and **2** complexes. However, those corresponding to C1−OH and C4−OH of A5P interact mainly with residues from the loop, including Arg63 that folds over the top of **2** in our structure. The results with the deoxy analogues therefore suggest that interaction with the initially disordered 147−152 turn is crucial for the proper recognition of A5P or its analogues by KDOPS and that some of the favorable binding energy may arise from interaction with, concomitant ordering of, and increased intramolecular hydrogen bonding within the strand that ends at this turn.

Second, while the openness of the region surrounding the C1 hydroxyl group predisposes KDOPS to be less sensitive to variation at this position in the substrate, this openness also provides sufficient free space to accommodate binding

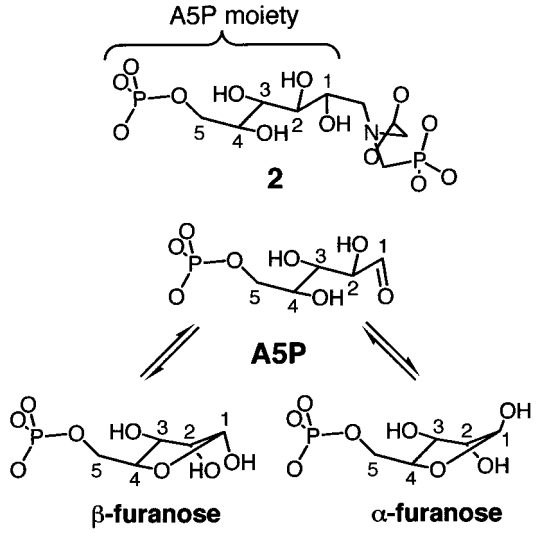

FIGURE 6: A5P moiety derived from the enzyme-bound inhibitor (**2**) structure is shown in mutarotation between its acyclic (aldehyde) and cyclic (α- and *β*-furanose) forms.

by the acyclic form of A5P or by either of A5P's cyclic furanose forms (Figure 6). Indeed, the C1, which represents the anomeric carbon of A5P, is only 3.6 Å away from the hydroxyl oxygen at C4 and is thus sufficiently close to rationalize KDOPS's recognition of the ring-opened form or of either furanose form. In addition, since the values of the rate constants for the ring opening of free A5P in solution are 1 order of magnitude greater than the k_{cat} for KDOPS (*7*), the enzyme need not activate bound anomeric forms of A5P for ring opening. Thus, if we assume that the position of the C1 hydroxyl of the A5P moiety in KDOPS·**2** closely mimics the position of the A5P carbonyl in its bound acyclic form (KDOPS·A5P), then KDOP's active site should allow the ring closure and the ring opening of A5P to proceed spontaneously, with little conformational mobility at the active site. A definitive confirmation of the A5P's binding features awaits the determination of the X-ray structure of a KDOPS·A5P complex; however, the present structural data in conjunction with our very recent observations by solid-state REDOR NMR (*14*) suggest that A5P's dynamic mutarotation (Figure 6), an interconversion between cyclic and acyclic forms, should be possible at the enzyme active site.

SUMMARY AND CONCLUSIONS

The two crystal structures of KDOPS that we present here illustrate the value of protein crystal structural analysis for characterizing the enzymatic reaction mechanism of KDOPS. Mechanistic hypotheses have underscored certain specifics of the interaction between the enzyme and the substrate, and these features in turn have provided further clarification of the details of the enzymatic reaction. The observed stereochemical preference for a distinct conformer of PEP suggests that the condensation step between PEP and A5P should proceed in a stepwise manner through the formation of a transient oxocarbenium ion at C2 of PEP. Comparison of the observed unique mode of binding by PEP to KDOPS with the mode of binding by PEP to the very closely related enzyme DAHPS suggests that their initial elementary steps of catalysis are different. This postulated mechanistic difference between these two enzymes can rationalize the unique requirement for metal ions by DAHPS, but not by KDOPS, even though the chemical reactions catalyzed by both enzymes appear to be remarkably similar.

ACKNOWLEDGMENT

We thank Profs. George Phillips (Rice University) and Florentine Quiocho (Baylor College of Medicine) for use of their X-ray data collection equipment and Dr. Craig Ogata for assistance with the use of beamline X4A at the National Synchrotron Light Source at Brookhaven National Laboratory.

REFERENCES

1. Ray, P. H. (1980) *J. Bacteriol. 141*, 635−644.
2. Unger, F. M. (1981) *Adv. Carbohydr. Chem. Biochem. 38*, 323−388.
3. Haslam, E. (1993) in *Shikimic Acid. Metabolism and Metabolites*, Wiley, New York.
4. Walsh, C. T., Benson, T. E., Kim, D. H., and Lees, W. J. (1996) *Chem. Biol. 3*, 83−91.
5. Anderson, K. S., and Johnson, K. A. (1990) *Chem. Rev. 90*, 1131−1149.
6. Brown, E., Marquardt, J., Lee, J., Walsh, C. T., and Anderson, K. S. (1994) *Biochemistry 33*, 10638−10645.
7. Kohen, A., Jakob, A., and Baasov, T. (1992) *Eur. J. Biochem. 208*, 443−449.
8. Kohen, A., Berkovich, R., Belakhov, V., and Baasov, T. (1993) *Bioorg. Med. Chem. Lett. 3*, 1577−1582.
9. Dotson, G. D., Nanjappan, P., Reily, M. D., and Woodard, R. W. (1993) *Biochemistry 32*, 12392−12397.
10. Liang, P., Lewis, J., Anderson, K. S., Kohen, A., D'Souza, W. F., Benenson, Y., and Baasov, T. (1998) *Biochemistry 37*, 16390−16399.
11. Du, S., Faiger, H., Belakhov, V., and Baasov, T. (1999) *Bioorg. Med. Chem. 7*, 2671−2682.
12. Hedstrom, L., and Abeles, R. (1988) *Biochem. Biophysics. Res. Commun. 157*, 816−820.
13. Kaustov, L., Kababya, S., Du, S., Baasov, T., Gropper, S., Shoham, Y., and Schmidt, A. (2000) *J. Am. Chem. Soc. 122*, 2649−2650.
14. Kaustov, L., Kababya, S., Du, S., Baasov, T., Gropper, S., Shoham, Y., and Schmidt, A. (2000) *Biochemistry 39*, 14865−14876.
15. Radaev, S., Dastidar, P., Patel, M., Woodard, R. W., and Gatti, D. L. (2000) *J. Biol. Chem. 275*, 9476−9484.
16. Shumilin, I. A., Kretsinger, R. H., and Bauerle, R. H. (1999) *Structure 7*, 865−875.
17. Wagner, T., Kretsinger, R. H., Bauerle, R. H., and Tolbert, W. D. (2000) *J. Mol. Biol. 301*, 233−238.
18. Mechaly, A., Teplinsky, A., Belakhov, V., Baasov, T., Shoham, G., and Shoham, Y. (2000) *J. Biotechnol. 78*, 83−86.
19. Otwinowski, Z. (1993) DENZO: An Oscillation Data Processing Program for Macromolecular Crystallography, Yale University Press, New Haven, CT.
20. Otwinowski, Z. (1993) SCALEPACK: Software for the Scaling Together of Integrated Intensities Measured on a Number of Separate Diffraction Images, Yale University Press, New Haven, CT.
21. Navaza, J. (1994) *Acta Crystallogr. A50*, 157−163.
22. Brunger, A. T. (1992) X-PLOR: A System for X-ray Crystallography and NMR, Yale University Press, New Haven, CT.
23. Burgi, H. B., Dunitz, J. D., Lehn, J. M., and Wipff, G. (1974) *Tetrahedron 30*, 1563−1572.
24. Baasov, T., and Kohen, A. (1995) *J. Am. Chem. Soc. 117*, 6165−6174.
25. Souhassou, M., Schaber, P. M., and Blessing, R. H. (1996) *Acta Crystallogr. B52*, 865−875.

26. Zhang, E., Brewer, J. M., Minor, W., Carreira, L. A., and Lebioda, L. (1997) *Biochemistry 36*, 12526−12534.
27. Benenson, Y., Belakhov, V., and Baasov, T. (1996) *Bioorg. Med. Chem. Lett. 6*, 2901−2906.
28. Du, S., Plat, D., Belakhov, V., and Baasov, T. (1997) *J. Org. Chem. 62*, 794−804.
29. Kim, D. H., Lees, W. J., Haley, T. M., and Walsh, C. T. (1995) *J. Am. Chem. Soc. 117*, 1494−1502.
30. Albeg, D. G., Lauhon, C. T., Nyfeler, R., Faasler, A., and Bartlett, P. A. (1992) *J. Am. Chem. Soc. 114*, 3535−3546.
31. Rose, I. A. (1972) *CRC Crit. Rev. Biochem. 1*, 33−57.
32. Matsumura, H., Tereda, M., Shirakata, S., Inoue, T., Yoshinaga, T., Izui, K., and Kai, Y. (1999) *FEBS Lett. 458*, 93−96.
33. Larsen, T. M., Laughlin, L. T., Holden, H. M., and Rayment, I. (1994) *Biochemistry 33*, 6301−6309.
34. Herzberg, O., Chen, C. C. H., Kapadia, G., Mcguire, M., Carroll, L. G., Noh, S. J., and Dunaway-Mariano, D. (1996) *Proc. Natl. Acad. Sci. U.S.A. 93*, 2652−2657.
35. DeLeo, A. G., Dayan, J., and Sprinson, D. B. (1973) *Biochem. Biophys. Res. Commun. 26*, 187−192.
36. Wagner, T., Shumilin, I. A., Bauerle, R., and Kretsinger, R. H. (2000) *J. Mol. Biol. 301*, 389−399.
37. Ray, P. H., Kelsey, J. E., Bigham, E. C., Benedict, C. D., and Miller, T. A. (1983) *ACS Symp. Ser. 231*, 141−170.

BI010339D